

UCRL- 96519
PREPRINT

UCRL--96519

DE88 001633

Resolution Limitations and
Optimization of the LLNL Streak
Camera Focus

R. A. Lerche
R. L. Griffith

This paper was prepared for submittal to
SPIE's 31st Annual International
Symposium, August 14-21, 1987, in
San Diego, California

September 1987

Lawrence
Livermore
National
Laboratory

This is a preprint of a paper intended for publication in a journal or proceedings. Since changes may be made before publication, this preprint is made available with the understanding that it will not be cited or reproduced without the permission of the author.

DISCLAIMER

This report was prepared as an account of work sponsored by an agency of the United States Government. Neither the United States Government nor any agency thereof, nor any of their employees, makes any warranty, express or implied, or assumes any legal liability or responsibility for the accuracy, completeness, or usefulness of any information, apparatus, product, or process disclosed, or represents that its use would not infringe privately owned rights. Reference herein to any specific commercial product, process, or service by trade name, trademark, manufacturer, or otherwise does not necessarily constitute or imply its endorsement, recommendation, or favoring by the United States Government or any agency thereof. The views and opinions of authors expressed herein do not necessarily state or reflect those of the United States Government or any agency thereof.

Resolution limitations and optimization of the LLNL streak camera focus*

R. A. Lerche and R. L. Griffith

Lawrence Livermore National Laboratory
University of California
P.O. Box 5508, L-473, Livermore, California 94550

ABSTRACT

The RCA C73435 image tube is biased at voltages far from its original design in the LLNL ultrafast (10 ps) streak camera. Its output resolution at streak camera operating potentials has been measured as a function of input slit width, incident-light wavelength, and focus-grid voltage. The temporal resolution is insensitive to focus-grid voltage for a narrow (100 μm) input slit but is very sensitive to focus-grid voltage for a wide (2 mm) input slit. At the optimum wide-slit focus voltage, temporal resolution is insensitive to slit width. Spatial resolution is nearly independent of focus-grid voltage for values that give good temporal resolution. Both temporal and spatial resolution depend on the incident-light wavelength. Data for 1.06- μm light show significantly better focusing than for 0.53- μm light. Streak camera operation is simulated with a computer program that calculates photoelectron trajectories. Electron ray tracing describes all of the observed effects of slit width, incident-light wavelength, and focus-grid voltage on output resolution.

1. INTRODUCTION

At the Lawrence Livermore National Laboratory (LLNL), ultrafast streak cameras are used by the Laser Fusion Program to record fast transient optical and x-ray signals.¹ Their temporal resolution is unmatched by any other transient recorder. Their ability to spatially discriminate an image along the input slit allows them to function as a one-dimensional image recorder, time-resolved spectrometer, or multichannel transient recorder. Depending on the choice of photocathode, they can be made sensitive to photon energies from 1.1 eV to 30 keV and beyond.

Most of the streak cameras used in the Laser Fusion Program are of an LLNL design. The optical cameras use the RCA C73435A image tube as the streak tube. The x-ray cameras use the same type image tube fitted with a special photocathode and extraction grid. Both cameras are typically operated with 100- μm wide input slits. This is to minimize the temporal broadening related to the image width of the slit. Several years ago an LLNL ultrafast streak camera fitted with a 1.5-mm wide slit recorded 1.06- μm laser pulses with no noticeable loss in temporal or spatial resolution.²

Recent applications requiring greater streak camera sensitivity caused us to carefully examine the effect of slit width, focus-grid voltage, and incident-light wavelength on streak camera resolution. We used static measurements, dynamic measurements, and computer modeling to develop an understanding of the focusing properties of the RCA C73435 series image tube operating as an ultrafast streak tube. Static measurements adequately describe all of the focusing properties of the camera. They are used to predict the dynamic response of the camera to short (1 ps) laser pulses. An electron ray tracing computer program was used to model the streak tube operation. The results of the modeling work predict the measured static characteristics and help us visualize the focusing properties of the tube. An understanding of these focusing properties allows us to recognize the limitations of the camera and to optimize its resolution for specific applications.

2. TYPICAL STREAK CAMERA OPERATION

Standard LLNL optical streak cameras like the one shown schematically in Fig. 1 were used for these studies. Incident light passes through band-pass and attenuating filters, then falls on a slit aperture whose width is adjustable from 50 μm to 2 mm. The slit is imaged onto the photocathode of the streak tube by a 1:l relay lens. Emitted photoelectrons are accelerated and focused at the tube's phosphor screen. Deflection plates sweep the image across the screen to provide a positional variation in intensity that corresponds to the time variation of the light intensity at the photocathode. A proximity focused microchannel plate (MCP) image intensifier tube (IIT) provides signal amplification for permanent recording on film or CCD array.

* Work performed under the auspices of the U.S. Department of Energy by the Lawrence Livermore National Laboratory under contract number W-7405-ENG-48.

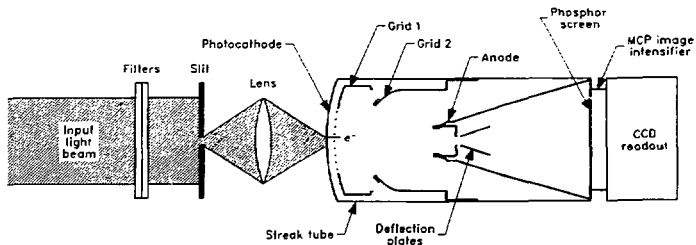


Figure 1. Schematic diagram of the LLNL streak camera.

2.1. Bias voltage

The RCA C73435 tube is designed to operate as an image tube.³ It is cylindrically symmetric except for the gating grid (Grid 1) and the deflection plates. The gating grid is a set of parallel wires spaced 5 mm apart 7 mm from the photocathode. The tube was designed to operate with its gating grid, focus grid (Grid 2), and anode nominally set at the voltages listed in Table 1. Removal of the gating grid has no effect on the image quality of the tube because it follows an equipotential surface of the tube built without it.⁴ The cathode, focus grid, and anode form a spherical lens that images photoelectrons from the photocathode to the phosphor screen.

Table 1. Nominal RCA C73435 image tube operating voltages.

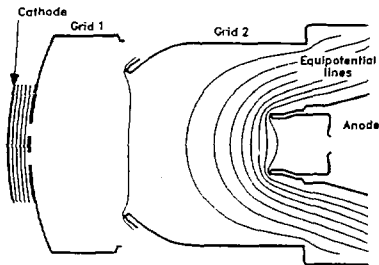
Electrode	Image Mode (volts)	Streak Mode (volts)
Cathode	0	0
Grid 1	150	2,500
Grid 2	1,700	875
Anode	15,000	17,000

Photoelectron transit-time spread through the tube limits the temporal resolution. It is inversely proportional to the electric-field strength at the photocathode surface. For ultrafast streak camera operation the extraction field is increased by applying a larger bias voltage between the gating grid and the photocathode. The gating grid now functions as an extraction grid. This destroys the axial symmetry of the electric field in the space around the extraction grid and forms a diverging, cylindrical lens for the photoelectrons.⁵ All photoelectrons except those originating in narrow strips of the photocathode midway between grid wires are deflected away from their normal paths through the anode aperture. The focus grid potential is adjusted to form the stronger positive lens required to focus the image of the input slit onto the phosphor screen. Typical bias voltages used in the LLNL cameras are listed in Table 1. (All voltages in this paper are given relative to the photocathode.) Figure 2 shows selected equipotential lines near the gating grid for normal imaging and ultrafast streaking operation.

2.2. Streak camera setup

During streak camera setup and calibration the input slit is illuminated with low level light. Adjustments are made to the camera while the image of the slit is monitored at the output of the IIT. First the slit is centered between the grid wires. Then the focus grid voltage is adjusted to provide the "best" static (non-swept) image of a resolution pattern placed in the plane of a 50- μ m-wide slit. Best focus occurs when the clearest visual image appears at the output of the IIT. An externally adjustable control allows the focus-grid voltage to be adjusted between 600 to 1250 volts. Best focus nominally occurs around 875 volts relative to the photocathode.

(a) Image mode



(b) Streak mode

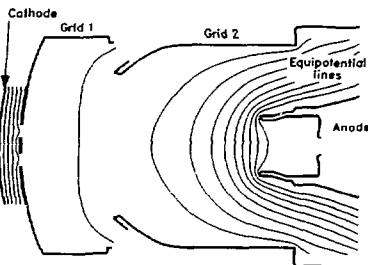


Figure 2. Plot of the equipotential lines in the region between the photocathode and the anode aperture. (a) Shows image mode operation with Grid 1, Grid 2, and anode set at 0.15, 1.7, and 15.0 kV, respectively. Equipotential lines are drawn at 30-volt intervals between the photocathode and Grid 1 and 1.5-kV intervals between Grid 1 and the anode. (b) Shows streak mode operation with Grid 1, Grid 2, and anode set at 2.5, 0.9, and 17.0 kV, respectively. Equipotential lines are drawn at 500-volt intervals between the photocathode and Grid 1 and at 1.7-kV intervals between Grid 1 and the anode. Note the cylindrical lens formed near Grid 1.

3. STREAK CAMERA FOCUSING PROPERTIES

Work to determine the focusing properties of the LLNL optical streak camera was done in three distinct stages: static measurements, dynamic measurements, and computer modeling. Static characterization refers to measurements taken while the streak camera is operating in its "pulsed" mode with the deflection plates grounded. Static characterization is much easier to perform than dynamic characterization. Its purpose is to predict the dynamic response (temporal resolution, spatial resolution, and onset of saturation) of the streak camera under nearly ideal conditions. The camera operates at its normal voltages with the IIT gated for 100 μ s. The output image can be formed with input power that varies by 7 orders of magnitude and the output image shape is independent of the input temporal shape. The experimental setup used for static characterization is shown in Fig. 1. For the static resolution measurements reported in this paper, the light source is an incandescent lamp with the appropriate band-pass filter. A CCD readout was used to enable rapid data analysis.⁶

3.1. Usable photocathode area

Streak camera input/output characteristics are shown in Fig. 3. They show the output signal amplitude and position plotted as a function of input slit position. These characteristics were measured by illuminating narrow strips of the photocathode with 1.06- μ m light and recording the output image. The data show the output amplitude to be nearly constant over the central 1.2 mm of the 5-mm space between grid wires. Only photoelectrons emitted from the narrow strip of the photocathode midway between grid wires reach the tube's phosphor screen. Data in Fig. 3b show that the image magnification along the temporal axis of the tube depends on the focus-grid voltage. At 875 volts, all input points focus to the same output point. This suggests that slit widths much greater than 100 μ m can be used to increase the usable area of the photocathode without degrading the temporal resolution.

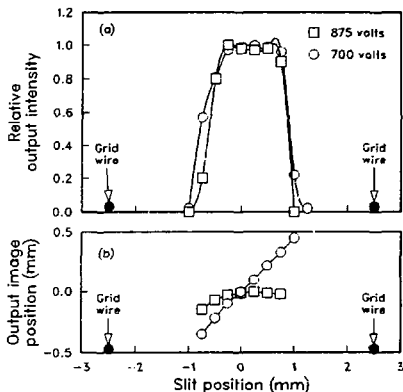


Figure 3. Streak camera input/output characteristics. The curves show (a) the relative output signal intensity and (b) the output image position versus input slit position for two focus-grid voltages. Data were recorded with a 200- μ m wide input slit.

3.2. Temporal resolution

Four factors determine the temporal resolution of a streak camera: static image width, sweep speed, photoelectron energy spread, and extraction field strength. The image width Δx and sweep speed S of the image along the temporal axis at the output of the tube determine the focus-limited temporal response Δt_x , which may be written as

$$\Delta t_x = \Delta x / S \quad (1)$$

The energy spread of photoelectrons simultaneously emitted from the photocathode results in a temporal spread in their arrival times at the phosphor screen. The extent of this transit-time spread Δt_t depends on the electric field strength E at the photocathode surface and the energy spread of the photoelectrons $\Delta \epsilon$. For our cameras most of the transit-time spread occurs while the electrons are near the photocathode and may be written as

$$\Delta t_t = 3.37 \times 10^{-8} \sqrt{\Delta \epsilon / E} \quad (2)$$

where Δt_t is in seconds, $\Delta \epsilon$ in eV, and E in volts/cm. The overall time response of the tube is the focus-limited response added in quadrature with the transit-time spread, that is

$$\Delta t = [(\Delta t_x)^2 + (\Delta t_t)^2]^{1/2} \quad (3)$$

Responses reported in this paper are given as full-width at half-maximum (FWHM) values.

The focus-limited temporal response of a streak camera can be estimated from the static image width and sweep speed using Eq. (1). Static image width data were recorded for four LLNL optical streak cameras. Figure 4 shows a typical set of data plotted as a function of three variables: input slit width, incident-light wavelength, and streak tube focus-grid voltage. The optimum focus voltage differs for the two slit widths. The sensitivity of the image width to focus voltage also differs greatly for the two slit widths. The image width of the 100- μ m slit is relatively insensitive to focus voltage while the 2-mm slit image is very sensitive to focus voltage. At the optimum wide slit focus voltage, the image width is insensitive to input slit width.

The features of the 0.53- and the 1.06- μm data are similar. However, the image width is greater for each 0.53- μm data point than for the corresponding 1.06- μm data point. This is attributed to a higher transverse photoelectron energy spread for 0.53- μm light. The energy of a 1.06- μm photon barely exceeds the work function of an S1 photocathode, so the resultant photoelectron has near-zero initial energy. The energy of a 0.53- μm photon, however, exceeds the work function by about 1.2 eV. This excess energy gives the photoelectrons an initial energy. Electron optic modeling matches the experimental results for 0.53- μm data when an initial transverse energy spread of 0.125 eV is used. Data taken with 0.40- μm light appears identical to the 0.53- μm data.

The dynamic response of a camera can be predicted from static data like that shown in Fig. 4. It can be determined by measuring its response to a very short pulse. Measurements were made using 1-ps, 0.59- μm dye laser pulses passed through a 1" etalon to produce a set of pulses spaced 169 ps apart. Figure 5 shows these dynamic pulse widths plotted with the predicted temporal response based on the 0.53- μm static image width data shown in Fig. 4 and the sweep speed value determined from the dynamic data. These predictions include the effect of a 10-ps transit-time spread estimated from the electric field strength at the photocathode and an axial energy spread of 1 eV.

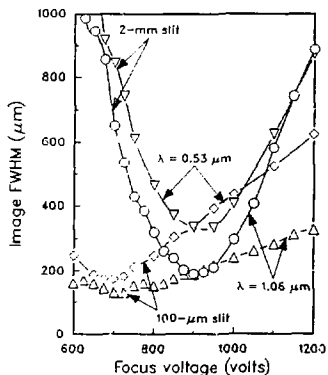


Figure 4. Static image width along the temporal axis versus focus-grid (Grid 2) voltage for 0.53- and 1.06- μm light. Data are presented for 100- μm and 2-mm wide slits. The streak tube has a S1 photocathode.

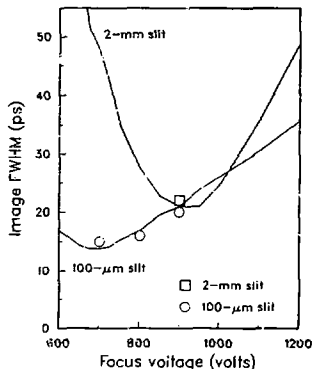


Figure 5. Measured and predicted temporal resolution. The data points represent dynamic measurements. The solid lines represent predictions based on the data presented in Fig. 4.

3.3. Spatial resolution

The camera's spatial resolution is determined from its point spread function (PSF). In static measurements, the PSF is formed by illuminating a 100- μm by 100- μm square aperture with a low intensity light source. The resulting image width, taken perpendicular to the sweep direction, is the spatial resolution of the camera. The spatial image width is plotted as a function of focus voltage in Fig. 6 for 0.53- and 1.06- μm light. The data show the spatial image width to be insensitive to the focus voltage but sensitive to photon wavelength. Image width does not show the actual shape of the lineouts. For these data, the lineouts appear Gaussian for 2 orders of magnitude except at extreme values of focus voltage range where they are slightly asymmetric.

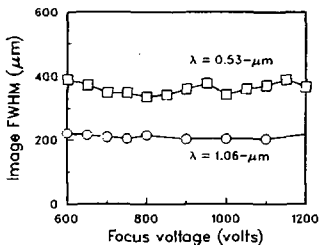


Figure 6. Streak camera spatial resolution versus focus-grid voltage for 0.53- and 1.06- μm light. The streak tube has a S1 photocathode.

4. MODELING STREAK CAMERA OPERATION

A modified version of Herrmannfeldt's electron trajectory computer program⁷ was used to model the effects of slit width, focus-grid voltage, and photoelectron energy on the streak tube resolution. Input to the program consists of electrode boundary conditions and initial conditions for selected electron trajectories. Graphic and tabular output includes electrode profiles, equipotential lines, electron trajectories, and electron transit times to the screen. To reduce the computational time needed to run the simulations, a few carefully selected trajectories are used to represent the spatial and energy distributions of the photoelectrons emitted from the photocathode.

The program allows the use of either cylindrical or rectangular symmetry, but not both. The image tube in streaked operation has rectangular symmetry between the cathode and extraction grid and makes a transition to cylindrical symmetry between the extraction grid and the focus grid. To model tube operation, the extraction grid opening is modeled as a 5-mm wide ring with a 5-mm inner diameter. The electric field distribution across the ring is nearly identical to that across a rectangular slot of equal width. The electric field after the extraction grid is virtually unaffected by the modeling of the slot. The analysis of the temporal and spatial focusing properties of the tube are treated as separate problems.

4.1. Focus-limited temporal response

For calculating the focus-limited image width parallel to the streak direction, the slit width is modeled by the starting coordinates of the selected electron trajectories. Trajectories starting from a single point on the photocathode simulate illumination through a narrow slit. Trajectories starting from a set of equally spaced points along the photocathode surface simulate illumination through a wide slit. See Figs. 7 and 8.

The velocity distribution of the photoelectrons emitted from the photocathode depends on the incident photon energy and the photocathode material. The image width in the temporal direction depends on the initial transverse velocity distribution of the photoelectrons while the transit-time spread between the photocathode and screen depends on the initial axial velocity distribution of the photoelectrons. Four trajectories from each starting point are used to model the velocity distributions. The transverse velocity distribution is modeled by two electrons started with equal energies but in opposite directions parallel to the photocathode surface. The axial velocity distribution is modeled by one electron with no initial energy and one with an axial energy equal to 70% of the photon energy above the photocathode work function.

Figure 7 shows electron trajectories that simulate the photocathode being illuminated through a narrow slit by light of several different wavelengths. The electrons emitted with different tangential energies focus to an image plane that coincides with the plane of the phosphor screen when the focus grid voltage is 700 volts. The image plane moves towards the photocathode for lower voltages and further away for larger voltages.

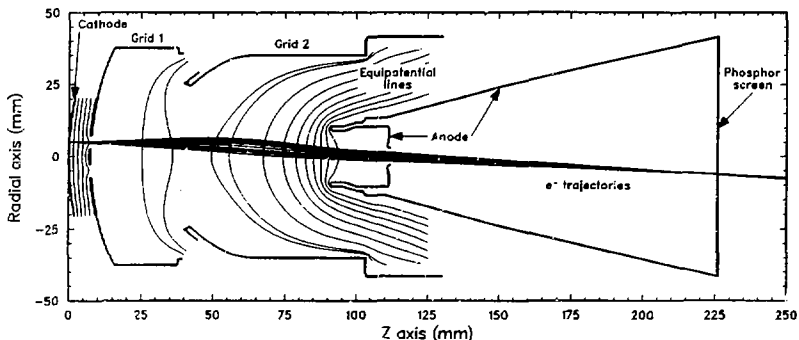


Figure 7. Electron trajectories for a narrow slit simulation of streak tube operation. The plot shows selected electron trajectories, equipotential lines, and electrode profiles. The trajectories start from a single point on the photocathode with different amounts of transverse energy. The extraction grid, focus grid, and anode are biased at 2.5, 0.7, and 17.0 kV, respectively. Trajectories are plotted for initial transverse electron energies of 0, 0.125, 0.25, 0.5, and 1.0 eV.

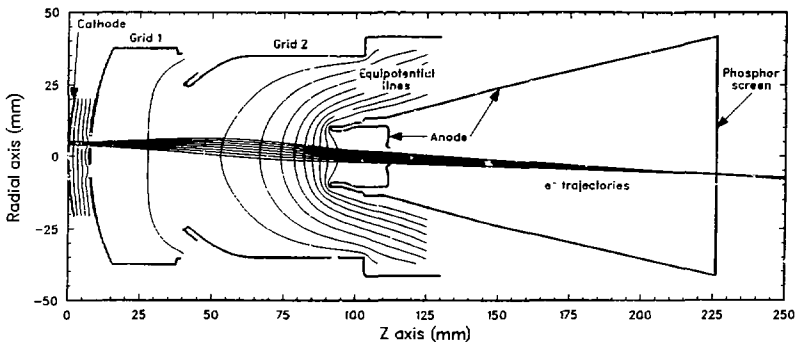


Figure 8. Electron trajectories for a wide slit simulation of streak tube operation. The plot shows selected electron trajectories, equipotential lines, and electrode profiles. The trajectories start from points uniformly spaced across the photocathode. The extraction grid, focus-grid, and anode are biased at 2.5, 0.9, and 17.0 kV, respectively. Trajectories are plotted for 0 eV electrons. Spacing between trajectory starting points is 200 μm .

Figure 9 shows the image width at the screen plotted as a function of focus-grid voltage for transverse energies of 0.03 and 0.125 eV. The optimum focus voltage is independent of the incident light wavelength. The exact voltage of the minimum shows a weak (50 volt) dependence on the position of the slit relative to the center of the extraction-grid opening. The image width is independent of wavelength at the optimum focus voltage. The slope of each curve away from the optimum focus voltage depends on the initial transverse energy distribution of the electrons. Greater transverse energy causes a greater slope. A transverse energy of 0.125 eV produces results similar to incident 0.53- μm light.

The electron trajectories shown in Fig. 8 simulate the photocathode being illuminated through a wide slit by photons with an energy equal to the work function of the photocathode. This is a reasonable approximation for electrons emitted from an Si photocathode by 1.06- μm light. Only trajectories starting from a 1.5-mm wide strip of the photocathode centered relative to the extraction-grid gap pass through the anode aperture to the phosphor screen. The electrons emitted from points within the 1.5-mm wide strip converge at a plane that coincides with the phosphor screen for a focus-grid voltage near 900 volts. The focal point moves towards the photocathode for lower voltages and further away for larger voltages. Figure 10 shows the image width of the wide slit plotted as a function of focus-grid voltage for transverse energies of 0.0 and 0.125 eV. The image width shows a strong dependence on focus-grid voltage and has its minimum at 900 volts. The 1.06- μm light produces a smaller image width than 0.53- μm light because the emitted electrons have a lower transverse electron energy.

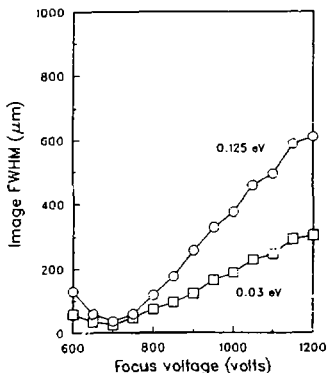


Figure 9. The focus-limited image width (temporal axis) versus focus-grid voltage for narrow slit operation predicted using electron trajectory calculations. Curves are presented for average transverse electron energy distributions of 0.03 and 0.125 eV.

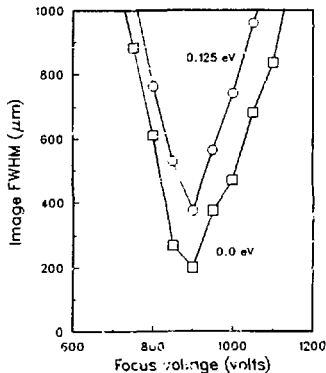


Figure 10. The focus-limited image width (temporal axis) versus focus-grid voltage for wide-slit operation predicted using electron trajectory calculations. Curves are presented for average transverse electron energy distributions of 0 and 0.125 eV.

4.2. Spatial resolution

The voltage applied to the extraction grid forms a cylindrical lens. Note that there is no transverse electric field perpendicular to the sweep direction in the space between the photocathode and extraction grid. Simulation of the spatial focusing is done by assuming the extraction grid is a fine mesh biased at a constant potential. Electron ray tracing shows that the spherical lens formed by the focus grid and anode is too weak to focus the photoelectrons in the spatial direction. The output spot size increases with increasing transverse energy of the photoelectrons. With the extraction grid voltage set at 2500 volts, the image width appears to be independent of the focus-grid voltage for values between 600 and 1200 volts.

5. SUMMARY

The focusing properties of the RCA C73435 image tube operating as an ultrafast streak tube are presented. They were measured using static techniques and include the dependence of temporal and spatial image width on input slit width, incident-photon energy, and focus-grid voltage. The static data are used to accurately predict the measured dynamic response of the camera to a 1-ps laser pulse. An electron ray tracing program is used to model the static operation of the tube. The simulations predict and explain the major features of the static characteristics.

For the bias voltages typically used with the LLNL streak camera, the temporal resolution is found to be insensitive to slit width, while the output-signal amplitude is proportional to slit width. Thus, wide (1000 μm) slits can be used to improve streak camera sensitivity without sacrificing temporal resolution. Also, a wider slit allows a lower photocathode current density to produce the same output signal amplitude. Some improvement in temporal response can generally be made by using a narrow (100 μm) slit and lowering the focus grid-voltage by 150 to 200 volts. Temporal resolution is relatively insensitive to focus voltage for a narrow slit, but not for a wide slit. The spatial resolution at focus-grid voltages that produce reasonable temporal focusing is nearly independent of the focus-grid voltage.

Both temporal and spatial resolution depend on the incident-light wavelength.

Streak camera operation is modeled with a computer program that calculates photoelectron trajectories. Simulations using selected electron trajectories describe all of the observed effects of slit width, incident-light wavelength, and focus-grid voltage on output image width. The focus-grid voltage controls the axial position of best temporal focus. It coincides with the phosphor screen at focus-grid values of 900 volts for a wide slit and 700 volts for a narrow slit. Lower voltages form a stronger electrostatic lens and move the image plane towards the photocathode. The temporal image width depends on the initial transverse energy of the photoelectrons parallel to the sweep axis of the tube while the spatial image width depends on the transverse energy perpendicular to the sweep axis of the tube.

6. ACKNOWLEDGMENTS

The authors would like to thank B. Jones for providing the CCD readout system and software that made gathering the experimental data possible and J. Wiedwald and D. Montgomery for many useful discussions concerning streak camera operation.

7. REFERENCES

1. L. W. Coleman, "Subnanosecond cinematography in laser fusion research: Current techniques and applications at the Lawrence Livermore National Laboratory," Proc. 16th Int'l Cong. on High Speed Photography and Photonics, (1984) SPIE Vol. 491, pp. 51-57.
2. Laser Program Annual Report - 1980, Lawrence Livermore National Laboratory, Livermore, California, UCRL-50021-80 (1981), pp. 5-19 to 5-21 (unpublished).
3. RCA specification sheet for the C73435 series image tube.
4. C. C. Lai, L. B. Olk, and R. D. Lear, "Photoelectron Trajectory Anatomy of RCA C73435 Image Converter and Its Performance," IEE Conference on Photoelectronic Imaging, Savoy Place, London, England, September 10-11, 1985. Also, Lawrence Livermore National Laboratory report, UCRL-91699, (1985).
5. R. C. Stoudenheimer, "Ultra-High Speed Streak Photography Using Image Tubes," RCA Application Note AN-4789 (1971).
6. B. A. Jones, "A lens coupled streak camera readout system utilizing a thermoelectric cooled CCD," Conf. on High Speed Photography, Videography and Photonics III, (1985) SPIE Vol. 569, pp. 189-193.
7. W. B. Herrmannsfeldt, "Electron Trajectory Program," Stanford Linear Accelerator Center, Stanford, California, SLAC-Report-226 (1979).